Accepted Manuscript

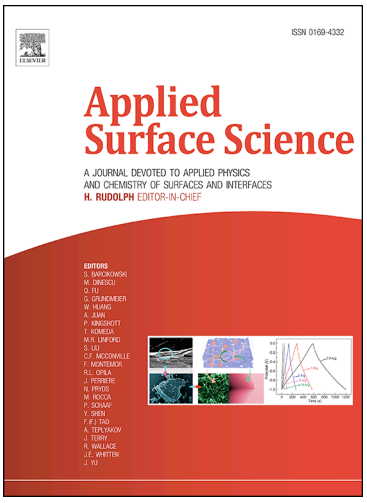

Full Length Article

The kinetic frictional shear stress of ZnO nanowires on graphite and mica substrates

Lizhen Hou, James Lee Mead, Shiliang Wang, Han Huang

PII: S0169-4332(18)32559-5
DOI: https://doi.org/10.1016/j.apsusc.2018.09.143
Reference: APSUSC 40447

To appear in: *Applied Surface Science*

Received Date: 29 June 2018
Revised Date: 24 August 2018
Accepted Date: 17 September 2018

Please cite this article as: L. Hou, J. Lee Mead, S. Wang, H. Huang, The kinetic frictional shear stress of ZnO nanowires on graphite and mica substrates, *Applied Surface Science* (2018), doi: https://doi.org/10.1016/j.apsusc.2018.09.143

The kinetic frictional shear stress of ZnO nanowires on graphite and mica substrates

Lizhen Hou [1,2], James Lee Mead,[1] Shiliang Wang[1,3,*], Han Huang[1,*]

1. *School of Mechanical and Mining Engineering, The University of Queensland, Brisbane, QLD 4072, Australia*
2. *School of Physics and Electronics, Hunan Normal University, Changsha 410081, China*
3. *School of Physics and Electronics, Central South University, Changsha, 410083, China.*

*Email: shiliang@mail.csu.edu.cn and han.huang@uq.edu.au

Abstract

The frictional shear stress between a nanostructure and a smooth substrate plays a crucial role in the development of nanodevices; however, it is extremely difficult to measure. In this work, the kinetic frictional shear stress of hexagonal ZnO nanowires on graphite and mica substrates was measured in an ambient atmosphere by optical microscope based nanomanipulation. Both substrates have similar surface roughness values of sub-angstrom-scale and interfacial adhesion energies with ZnO nanowires. Yet, a kinetic frictional shear stress of 0.51 MPa was obtained for the ZnO-graphite system, significantly lower than that of 5.1 MPa for the ZnO-mica system. The results demonstrate that the kinetic friction at a perfectly smooth contact interface may not be controlled by the adhesion, whilst being commonly referred to as adhesive friction or adhesion-dominated fiction. Similar to the combining equations for adhesion, we propose two empirical combining equations to estimate the frictional shear stress between two smooth surfaces using results more simply obtained from a reference surface. The validity of the equations is supported by our experimental results and recently published data for atomically smooth interface systems obtained under the similar environmental conditions.

Keywords:

Frictional shear stress, ZnO nanowires, graphite, mica, nanomanipulation, combining equation

1. Introduction

Nanoscale friction can significantly affect the design and performance of micro/nano-electro-mechanical systems [1], the assembly and manipulation of nanoparticles (NPs) and nanowires (NWs) [2-4], and the development of reversible dry adhesives [5] and wall-climbing robots [6]. As a result, an increasing number of studies over the past two decades have aimed to develop a fundamental understanding of nanoscale friction. In particular, rapid developments in atomistic simulations and atomic force microscopy (AFM) measurements have dramatically improved our understanding of nanoscale friction [7, 8]. Nevertheless, a large gap still exists between the newly acquired knowledge of nanoscale friction and the well-established theory of macroscale friction. Attempts to bridge this gap have been hindered by the inherent limitations of current simulation approaches [7] and measurement tools [8]. In regards to experimental limitations, the real contact area between an AFM tip and a target substrate is crucial for determining the nanoscale fiction, but is difficult to precisely determine [8, 9]. In addition, most AFM tips have amorphous or disordered tip ends, and thus are not suitable for characterizing the effects related to the localized atomic ordering such as the superlubricity or structural lubricity between crystalline surfaces [8, 9].

In the past decade, AFM based nanomanipulation was largely used to test nanoscale friction, as it is capable of achieving well-defined interfacial contact [10-16]. In such a test, a faceted nano-object, NP or NW, is pushed to slide along an atomically smooth substrate surface using an AFM tip, and the friction force between the object and substrate is detected by the AFM instrumentation [8]. As the contact area, surface texture and testing environment are well-defined, many significant results were obtained using the AFM based method, e.g. the identification of anisotropy and duality of the friction between atomically smooth crystalline surfaces [15, 16]. Recently, scanning electron microscopy (SEM) based nanomanipulation has also been developed as an alternative for measuring nanoscale friction [17]. This technology enables direct visualization of the testing process, and thus removes many of the testing uncertainties associated with AFM-based manipulation [17]. However, electron-beam induced effects can alter the molecular interactions at a nanoscale interface, so the friction

behavior observed during test differs from what would occur in ambient atmosphere conditions [3, 18]. To overcome the hurdles encountered during AFM and SEM-based tests, optical microscope (OM) based nanomanipulation was recently developed for characterizing the friction between NWs and substrates [19-21]. In this method, the friction force at a NW/substrate interface is derived from the bent profile of a NW that is pushed to slide on the substrate at a constant speed. As the entire testing process is monitored real time, it combines the advantages of both AFM and SEM-based tests.

Extensive experimental studies have demonstrated that the friction law at the nanoscale can be written as, $F_{\mathrm{k}} = \mu F_{\mathrm{N}} + \tau A$, where F_{k}, μ, F_{N}, τ, and A are the friction force, friction coefficient, external normal force, frictional shear stress, and contact area, respectively [22-24]. If no external normal forces are applied to the contact interface, i.e. $F_{\mathrm{N}} = 0$, the friction force, $F_{\mathrm{k}} = \tau A$, is known as adhesive friction or adhesion-dominated friction. Fundamentally, τ originates from atomic interactions that occur between contact surfaces [25], and is believed to be related to the interfacial adhesion force [22, 23]. However, a complete understanding of τ is yet to be established. For example, theoretical calculations and simulations based on the lattice interaction between two surfaces can qualitatively explain the anisotropy and duality of frictional forces [16, 26-28]. Yet, they cannot quantitatively interpret the experimental values obtained experimentally in a specific test [16, 26-28]. Although a number of results on the friction of well-defined interfaces were experimentally obtained, no relations have been established to predict the friction force between atomically flat surfaces without an externally applied normal force. This is quite different from the study of adhesion, where a class of empirical expressions, known as combining relations or combining laws, have been proposed for obtaining the approximate interfacial adhesion energies (forces) of various contact interfaces [23].

In the present work, we comparatively studied the kinetic frictional shear stress of ZnO NWs on cleaved graphite and mica substrates using the OM-based nanomanipulation technique developed in our group [19-21]. In our tests, the friction force of ZnO NWs on atomically smooth surfaces of

graphite and mica was measured under the same environmental conditions. Two empirical relationships were proposed to phenomenologically interpret the measured friction stress values of the two interfacial systems. The proposed combining relationships were also validated using recently published data of various interface systems.

2. Experimental

ZnO NWs were synthesized on a Si wafer by catalyst-free chemical vapour deposition (CVD) [29]. The morphology and structure of the NWs were characterized by SEM (JEOL JSM-7800F, operated at 10 kV) and transmission electron microscopy (TEM; FEI Tecnai F20 operated at 200 kV). Both the graphite and mica substrates were cleaved using tape immediately prior to friction testing. The ZnO NWs were directly transferred from the Si wafer onto the graphite or mica substrates, and then broken into short NW segments using the OM nanomanipulation technique developed in our previous studies [30, 31]. This process avoids the absorption of contaminants onto the surface of NW during transfer [32], as no additional liquids or adhesives are required. Kinetic friction testing was performed using the midpoint push test under an OM (Objective lens: Mitutoyo M Plan APO 100× with a resolution of 0.4 μm) in an ambient environment (temperature: ~25 ºC; relative humidity: 45 - 55 %). In the test, the NW was pushed laterally at its midpoint by a sphero-conical W tip (diameter: 150 - 400 nm) obtained by electrochemical etching method, to slide along the substrate at a constant speed. The kinetic frictional force was derived from the bent profile of the NW, obtained from *in situ* OM observation [19, 20]. The surface topography of the substrates and sizes of the NWs being tested were examined right after testing, using atomic force microscopy (AFM, Oxford Instruments Asylum Research, USA) and SEM.

3. Results and discussion

Figure 1(a) shows a low-magnification SEM image of the ZnO NWs grown on a Si wafer using catalyst-free CVD. The NWs have lengths of up to 100 μm. TEM analysis reveals that the NWs have a perfect single-crystalline structure, grown along the [001] direction, as shown in Figs. 1(b) and (c).

AFM analyses indicate that graphite and mica substrates exhibit average roughness values (R_a) of 0.05 and 0.04 nm, respectively (Figs. 2(a) and (b); scanning size: 10 × 10 μm). The mica substrate surface contains randomly scattered islands with a diameter of ~ 2 nm and a height of ~ 0.4 nm, which are presumed to be single atomic layers of potassium carbonate resulting from the reaction of carbonaceous gases and potassium ions [33]. Fig. 2(c) presents an AFM image of a typical ZnO NW with an atomically smooth surface.

Figure 3 shows the OM micrographs of a ZnO NW as it is pushed along the graphite substrate. Fig. 3(a) displays the NW laid on the substrate prior to sliding, with a W tip in contact near the midpoint of the NW. The tip then pushed the NW laterally, causing it to slide along the substrate at a constant speed. The NW would maintain a bent profile during pushing as the frictional force is distributed along its length (Fig. 3(b)). Adjustments were made during pushing to maintain lateral motion of the NW and to ensure sliding reached a steady state, as shown in Figure 3(c). After withdrawal of the tip, the bent profile of the NW was maintained due to the existence of static frictional force, as shown in Fig. 3(d).

To obtain the steady state shown in Fig. 3(c), a balance between the kinetic frictional force and elastic restoring force caused by bending of the NW must be reached. As the NW is flexible and the surfaces of the NW and substrate are perfectly smooth, it is assumed that the normal component of force applied by the tip during pushing of the NW acted only at its midpoint. This is expected to induce a normal stress in a highly localized area of the NW-substrate interface. In other words, the normal force component would have a negligible influence on the interfacial friction, except in the very vicinity of the midpoint. To verify this assumption, a three-dimensional (3D) axisymmetric finite element model (FEM) of the tip-NW-substrate system was developed. Based on SEM analysis, the sphero-conical W tip was modelled as a hemisphere of 400 nm in diameter, and the side-length of the hexagonal cross-section of a ZnO NW was set as 200 nm, as shown in Fig. 4. A 2 μm long segment of the NW was modelled on each side of its midpoint, and the NW-substrate interface was

perfectly smooth. The elastic moduli for the substrate, NW and tip were 24.1GPa [34], 140 GPa [29], and 410 GPa [35] respectively, and Poisson's ratios were all 0.3. All three components were meshed with SOLID 185 elements. Adjacent surfaces of tip and NW, and substrate and NW were modelled as Herztian contact pairs. During FEM simulation, a vertical load was applied by the tip, with a magnitude corresponding to a maximum contact pressure of 10 GPa, equal to the fracture strength of the NW [29]. As expected, the normal compressive stress experienced at the NW-substrate interface reached a maximum of 70 MPa at the NW's midpoint, and fell abruptly below 1 MPa at distance of just 1 μm from the midpoint. Those values are much smaller than the value of ~ 1 GPa, estimated by van de Waals (vdW) force [23], $F_{\mathrm{vdw}} = A_{12}/6\pi {D_0}^3$, where A_{12} is the Hamaker constant of the NW-substrate system and can be approximated as $A_{12} = \sqrt{A_1 \cdot A_2}$ with $A_1 = 29 \times 10^{-20}$ Joules for graphite and $A_2 = 9.2 \times 10^{-20}$ Joules for ZnO, and $D_0 \approx 0.2$ nm is the cut-off distance. The simulation confirms that applying a normal force to a NW during pushing should negligibly influence the interfacial friction stress of the NW.

Based on the simulationed results, the bent profile of a NW can be approximated as a well-clamped cantilever beam under a uniformly distributed load, f, i.e. the kinetic friction force per unit length on the NW [20]. According to the elastic beam theory, f can be estimated by [19],

$$f = \begin{cases} 8 \cdot (\delta/L) \cdot (EI/L^3), & \delta/L \le 0.27, \\ \left[0.8263e^{3.645\delta/L} + 7.948 \cdot 10^{-11} \cdot e^{29.18\delta/L}\right](EI/L^3), & \delta/L > 0.27, \end{cases} \quad (1)$$

where E, I, L, and δ are the elastic modulus, area moment of inertia, half length, and deflection of the NW, respectively. For the ZnO NWs being tested, $E = 140$ GPa and $I = 5\sqrt{3}D^4/256$ were used [29], while the diameter, D, and length, L, of the NW were measured by SEM. The frictional shear stress, τ, i.e. the friction force per contact area, was therefore obtained from: $\tau = 2f/D$.

The optical image in Fig. 5(a) shows the bent profile of a ZnO NW when sliding steadily on a graphite substrate, where the deflection was measured as 4.4 ± 0.2 μm. The NW has a length of 16.78 ± 0.05 μm and diameter of 156 ± 3 nm, as shown in Fig. 5(b). Using Eq. (1), the frictional shear

stress was calculated as 0.34 ± 0.04 MPa. To validate the result, the bent profile of the NW was simulated using a FEM, meshed with SOLID 185 elements [36, 37]. Bending was induced in the NW model by enforces different frictional shear stress values of 0.30, 0.34 and 0.40 MPa, and the resulting bent profiles were plotted in Fig. 5(a). A frictional shear stress of 0.34 MPa provided a bent curve most closely matching the observed profile. To quantify the error, we extracted the data points for the NW profile using DataThief software [21], and found that R-squared value between the data points and the modelled curve is 0.9999. Fig. 5(a) also shows that the simulated NW profiles for 0.30 and 0.40 MPa deviate obviously from the observed profile, indicating the resolution of our OM based method provides sufficiently accurate measure of frictional shear stress. In this work, we tested 8 ZnO NWs on the graphite substrate and plotted the results as a function of NW diameter in Fig. 5(c). The frictional shear stresses varied from 0.33 to 0.75 MPa, giving an average value of 0.51 MPa with a standard deviation of 0.15 MPa. In addition, the frictional shear stress appears independent of the diameter of NWs, which ranged from 130 to 600 nm.

Similarly, the values of frictional shear stress between ZnO NWs and a mica substrate were determined. Fig. 6(a) shows a typical optical image of a NW, with a length of 17.89 μm and diameter of 447 nm, sliding on a mica substrate. Using Eq. (1), the frictional shear stress was calculated as 4.0 ± 0.4 MPa. Again, the bent profiles for friction stress values of 3.0, 4.0 and 5.0 MPa were simulated by FEM, as plotted in Fig. 6(a). The simulated profile for 4.0 MPa clearly matches well with the actual profile, and the corresponding R-squared value between the NW profile and the modelled curve is 0.999. We tested 12 NWs on the mica substrate, and plotted the results as a function of NW diameter in Fig. 6(b). The frictional shear stresses ranged from 3.0 to 7.5 MPa, giving an average value of 5.1 MPa with a standard deviation of 1.6 MPa. The frictional shear stress also appears to be independent of the diameter of the NWs. It should be noted that the cross sections of the NWs were supposed to be regular hexagons in our calculations due to the significant difficulties in the exact characterization. However, the true cross sections might be deviated from the regular ones, as can be seen from the SEM image in Fig. 6(a), where the top edge and two side-edges are 209, 120, 118 nm,

respectively. This should be an important error source for the considerable variation of the shear stress values for the NW-substrate systems. In addition, the surface contaminations formed or absorbed on the surfaces of NWs [18] and substrate surfaces [33] under the ambient atmosphere may also lead to the variation in the measured frictional shear stress values .

Although both NW-substrate systems have atomically smooth surfaces, the frictional shear stress of the ZnO-mica system is one order greater than that of the ZnO-graphite system. In an effort to understand why the two systems exhibit vastly different friction behaviour, we first consider the influence of interfacial adhesion energies (forces). Nanoscale friction without external normal load is often known as adhesive friction or adhesion-dominated friction, and hence is considered to correlate with adhesion energy [22-24]. The adhesion energy of a ZnO-graphite and ZnO-mica interfaces studied here have not be experimentally measured. However, the adhesion energy, or work of adhesion, W_{A-B}, for an interface that consists of two perfectly smooth surfaces, A and B, can be estimated by the combining relation [23],

$$W_{A-B} \approx \sqrt{W_{A-A} W_{B-B}}, \tag{2}$$

where W_{A-A} and W_{B-B} are the adhesion energies of $A-A$ and $B-B$ interfaces, respectively. The works of adhesion for graphite-graphite and mica-mica interfaces, W_{G-G} and W_{M-M}, can be used to estimate the difference in the works of adhesion of the systems studied here, as they both use the same ZnO NWs. The experimentally measured values for W_{G-G} and W_{M-M} are very close, 0.227 J m^{-2} [38] and 0.246 - 0.314 J m^{-2} [39], respectively. According to Equation (2), the difference in adhesion energies, and thus adhesion forces, between the two NW-substrate systems should be small. Therefore, the significant difference in frictional shear stress of the two NW-substrate systems could not be attributed to the difference between their adhesion energies [22-24].Theoretically, the friction and adhesion forces between two perfectly smooth surfaces in contact should stem from interfacial molecular interaction, however, they can differ in their interaction potentials [23, 40]. For mica surface, it was reported that the naturally present K^+ surface ions play an important role on its

tribological properties [41]. The surface ions might be also the main reason for the different frictional stress values between the atomically smooth NW-substrate interfaces.

It is well established that the work of adhesion for an *A*-*B* interfacial system can be estimated using Eq. (2). Similarly, provided that the sliding process in an *A*-*B* system is quasi-static, and that the energy is only dissipated by the lattice vibrations of each surface, we can define a work of friction, Γ_{A-B}, for the system, that should have similar combining relation to that defined by Eq. (2), expressed as,

$$\Gamma_{A-B} \approx \sqrt{\Gamma_{A-A}\Gamma_{B-B}}, \tag{3}$$

where Γ_{A-A} and Γ_{B-B} are the works of friction for *A*-*A* and *B*-*B* interfacial systems, respectively. The frictional shear stress for the *A*-*B* system, τ_{A-B}, should have the same form of relation as that in Eq. (3), written as,

$$\tau_{A-B} \approx \sqrt{\tau_{A-A}\tau_{B-B}}, \tag{4}$$

where τ_{A-A} and τ_{B-B} are the frictional shear stress values for *A*-*A* and *B*-*B* systems, respectively. This indicates that if the frictional shear stress values for *A*-*A* and *B*-*B* systems are known, the frictional shear stress for *A*-*B* can be calculated using Eq. (4). For surface *C* sliding on *A* and *B*, we thus have $\tau_{A-C} = \sqrt{\tau_{A-A}\tau_{C-C}}$, and $\tau_{B-C} = \sqrt{\tau_{B-B}\tau_{C-C}}$, so,

$$\tau_{A-C}/\tau_{B-C} \approx \sqrt{\tau_{A-A}/\tau_{B-B}}, \tag{5}$$

where τ_{A-C} and τ_{B-C} are the frictional shear stress values for *A*-*C* and *B*-*C* interfacial systems, respectively. The obtained combining relations were tested using our experimental measurement. Table 1 summarizes the measured frictional shear stress/force values and the combining relationship ratios for our experimental data as well as in recent literature. In our test, $\tau_{ZnO-M} = 5.1\,MPa$, $\tau_{ZnO-G} = 0.51\,MPa$, so $\tau_{ZnO-M}/\tau_{ZnO-G} = 10$. The frictional shear stress values for air-cleaved mica-mica and graphite-graphite without external normal force, and in an ambient atmosphere condition are $\tau_{M-M} \approx 7.5$ MPa [42] and $\tau_{G-G} \approx 0.05$ MPa [38], so $\sqrt{\tau_{M-M}/\tau_{G-G}} \approx 12$. The similar obtained ratios help to validate the use of Eq. (5). The ratios also agree well with result obtained from

previous tests of mica and graphite surfaces [43], where the frictional force between a Si AFM tip and a mica surface was 10 times higher than between the Si tip and graphite substrate (using an extremely low load in ambient atmosphere condition, see Table 1 for details).

Understanding the kinetic frictional behavior of two perfectly smooth surfaces is critical for the development of nanotechnology based devices, but quantifying friction shear stress remains a significant challenging. Atomically smooth surfaces often include the faceted surface of a NP or NW, the cleaved surface of a layered material, and the interlayers in a vdW heterostructure. The empirical combining relations, presented as Eqs. (4) and (5), appear to be useful in estimating the frictional shear stress of two contacting surfaces using relations obtained from previously tested alternative systems. For example, the frictional shear stress between a Sb NP and a cleaved MoS_2 surface can be deduced using the previous test results obtained from Sb NPs on a cleaved graphite substrate. We know the frictional shear stress for air-cleaved graphite-graphite and MoS_2-MoS_2 in high vacuum, $\tau_{G-G} \approx 0.02 - 0.04$ MPa [44], and $\tau_{MoS_2-MoS_2} \approx 0.02 - 0.06$ MPa [45], respectively, therefore $\tau_{G-G} \approx \tau_{MoS_2-MoS_2}$. Also, we know $\tau_{Sb-G} = 1.04$ MPa [16] in high vacuum. So Eq. (5) would suggest that $\tau_{Sb-MoS_2} \approx \tau_{Sb-G} \approx 1$ MPa. Indeed, in the same testing conditions, $\tau_{Sb-MoS_2} \approx 1$ MPa has been experimentally obtained [28]. This result is also verified by experiments involving the sliding of a Si AFM tip on both graphite and MoS_2 layers under the same testing conditions, where the same friction force of ~ 1 nN was obtained [46], i.e. $\tau_{Si-G}/\tau_{Si-MoS_2} = \sqrt{\tau_{G-G}/\tau_{MoS_2-MoS_2}} = 1$, again satisfying Eq. (5).

4. Conclusions

The kinetic frictional shear stress of hexagonal ZnO NWs sliding on cleaved graphite and mica substrates was measured in an ambient atmosphere using OM-based nanomanipulation. The mica and graphite substrates have sub-angstrom-scale surface roughness, and the NW-graphite and NW-mica interfaces have similar interfacial adhesion energies. The frictional shear stress for the NW-graphite system is 0.51 ± 0.15 MPa, one order lower than that of 5.1 ± 1.6 MPa for the NW-mica system. Our

results demonstrate that the adhesion behaviour of a perfectly smooth contact interface does not necessarily correlate with its kinetic frictional behaviour.

We proposed empirical combining relations for the frictional shear stresses exhibited by different contact interface systems when no external normal force is applied, i.e. the frictional shear stress of smooth surface *A* sliding on surface *B* related to the frictional shear stress values of *A*-*A* and *B*-*B*. The equations were validated using the results obtained in this work as well as from some other atomically smooth interface systems tested previously. If established, the use of the formulae could significantly reduce the number of experimental tests required to develop an understanding of an interfacial system's kinetic frictional behavior, and hence benefit the design of micro/nano-electro-mechanical systems.

Acknowledgments

This project is financially supported by the National Natural Science Foundation of China (No. 11502080, 11674399) and Australian Research Council (DP160103190). The authors would like to acknowledge the Australian National Fabrication facility (Queensland Node) for AFM characterization.

References

[1] B. Bhushan, Nanotribology and nanomechanics of MEMS/NEMS and BioMEMS/BioNEMS materials and devices. Microelectron. Eng. 84 (2007) 387-412.

[2] D. Dietzel, U. Schwarz, A. Schirmeisen, Nanotribological Studies by Nanoparticle Manipulation, in: E. Gnecco, E. Meyer (Eds.) Fundamentals of Friction and Wear on the Nanoscale, Springer International Publishing, 2015, pp. 363-393.

[3] B. Polyakov, L. Dorogin, S. Vlassov, I. Kink, R. Lõhmus, Tribological Aspects of In Situ Manipulation of Nanostructures Inside Scanning Electron Microscope, in: E. Gnecco, E. Meyer (Eds.) Fundamentals of Friction and Wear on the Nanoscale, Springer International Publishing, 2015, pp. 395-426.

[4] D. Maharaj, B. Bhushan, Nanomanipulation and Nanotribology of Nanoparticles and Nanotubes Using Atomic Force Microscopy, in: B. Bhushan, D. Luo, S.R. Schricker, W. Sigmund, S. Zauscher (Eds.) Handbook of Nanomaterials Properties, Springer Berlin Heidelberg, 2014, pp. 299-315.

[5] L.F. Boesel, C. Greiner, E. Arzt, A. del Campo, Gecko-Inspired Surfaces: A Path to Strong and Reversible Dry Adhesives. Adv. Mater. 22 (2010) 2125-2137.

[6] M.P. Murphy, C. Kute, Y. Mengüç, M. Sitti, Waalbot II: Adhesion Recovery and Improved Performance of a Climbing Robot using Fibrillar Adhesives. Int. J. Robot. Res. 30 (2011) 118-133.

[7] A. Vanossi, N. Manini, M. Urbakh, S. Zapperi, E. Tosatti, Colloquium: Modeling friction: From nanoscale to mesoscale. Reviews of Modern Physics 85 (2013) 529-552.

[8] D. Dietzel, U. Schwarz, A. Schirmeisen, Nanotribological studies using nanoparticle manipulation: Principles and application to structural lubricity. Friction 2 (2014) 114-139.

[9] Y. Mo, K.T. Turner, I. Szlufarska, Friction laws at the nanoscale. Nature 457 (2009) 1116-1119.

[10] E. Meyer, R. Overney, D. Brodbeck, L. Howald, R. Luthi, J. Frommer, H.J. Guntherodt, Friction and Wear of Langmuir-Blodgett-Films Observed by Friction Force Microscopy. Phys. Rev. Lett. 69 (1992) 1777-1780.

[11] R. Lüthi, E. Meyer, H. Haefke, L. Howald, W. Gutmannsbauer, H.-J. Güntherodt, Sled-Type Motion on the Nanometer Scale: Determination of Dissipation and Cohesive Energies of C60. Science 266 (1994) 1979-1981.

[12] M.R. Falvo, R.M. Taylor Ii, A. Helser, V. Chi, F.P. Brooks Jr, S. Washburn, R. Superfine, Nanometre-scale rolling and sliding of carbon nanotubes. Nature 397 (1999) 236-238.

[13] D. Dietzel, T. Monninghoff, L. Jansen, H. Fuchs, C. Ritter, U.D. Schwarz, A. Schirmeisen, Interfacial friction obtained by lateral manipulation of nanoparticles using atomic force microscopy techniques. J. Appl. Phys. 102 (2007) 084306-084311.

[14] H.J. Kim, K.H. Kang, D.E. Kim, Sliding and rolling frictional behavior of a single ZnO nanowire during manipulation with an AFM. Nanoscale 5 (2013) 6081-6087.

[15] P.E. Sheehan, C.M. Lieber, Nanotribology and nanofabrication of MoO3 structures by atomic force microscopy. Science 272 (1996) 1158-1161.

[16] D. Dietzel, C. Ritter, T. Monninghoff, H. Fuchs, A. Schirmeisen, U.D. Schwarz, Frictional duality observed during nanoparticle sliding. Phys. Rev. Lett. 101 (2008) 125505.

[17] L.M. Dorogin, S. Vlassov, B. Polyakov, M. Antsov, R. Lõhmus, I. Kink, A.E. Romanov, Real-time manipulation of ZnO nanowires on a flat surface employed for tribological measurements: Experimental methods and modeling. physica status solidi (b) 250 (2013) 305-317.

[18] J.L. Mead, H. Xie, S. Wang, H. Huang, Enhanced adhesion of ZnO nanowires during in situ scanning electron microscope peeling. Nanoscale 10 (2018) 3410 - 3420.

[19] H. Xie, S. Wang, H. Huang, Characterising the nanoscale kinetic friction using force-equilibrium and energy-conservation models with optical manipulation. Nanotechnology 27 (2016) 065709.

[20] S. Wang, L. Hou, H. Xie, H. Huang, The kinetic friction between a nanowire and a flat substrate measured using nanomanipulation with optical microscopy. Appl. Phys. Lett. 107 (2015) 103102.

[21] L. Hou, S. Wang, H. Huang, A simple criterion for determining the static friction force between nanowires and flat substrates using the most-bent-state method. Nanotechnology 26 (2015) 165702.

[22] B.N.J. Persson, Sliding Friction: Physical Principles and Applications, Springer Berlin Heidelberg, 2013.

[23] J.N. Israelachvili, Intermolecular and Surface Forces, Elsevier Science, 2010.

[24] B. Bhushan, Nanotribology and Nanomechanics: An Introduction, Springer Berlin Heidelberg, 2008.

[25] M. Hirano, K. Shinjo, Atomistic Locking and Friction. Phys. Rev. B 41 (1990) 11837-11851.

[26] M. Hirano, K. Shinjo, R. Kaneko, Y. Murata, Anisotropy of frictional forces in muscovite mica. Phys. Rev. Lett. 67 (1991) 2642-2645.

[27] M. Dienwiebel, G.S. Verhoeven, N. Pradeep, J.W.M. Frenken, J.A. Heimberg, H.W. Zandbergen, Superlubricity of Graphite. Phys. Rev. Lett. 92 (2004) 126101.

[28] D. Dietzel, J. Brndiar, I. Štich, A. Schirmeisen, Limitations of Structural Superlubricity: Chemical Bonds versus Contact Size. ACS Nano 11 (2017) 7642–7647.

[29] A. Roy, J. Mead, S. Wang, H. Huang, Effects of surface defects on the mechanical properties of ZnO nanowires. Sci. Rep. 7 (2017) 9547.

[30] S. Wang, Y. Wu, L. Lin, Y. He, H. Huang, Fracture Strain of SiC Nanowires and Direct Evidence of Electron-Beam Induced Amorphisation in the Strained Nanowires. Small 11 (2015) 1672–1676.

[31] S. Wang, Y. He, H. Huang, J. Zou, J.G. Auchterlonie, L. Hou, B. Huang, An improved loop test for experimentally approaching the intrinsic strength of alumina nanoscale whiskers. Nanotechnology 24 (2013) 285703.

[32] S. Wang, Q. Huang, Y. Wu, H. Huang, Unique structure and surface-related elastic modulus of alumina nanobelts. Nanotechnology 27 (2016) 475701.

[33] F. Ostendorf, C. Schmitz, S. Hirth, A. Kühnle, J.J. Kolodziej, M. Reichling, Evidence for Potassium Carbonate Crystallites on Air-Cleaved Mica Surfaces. Langmuir 25 (2009) 10764-10767.

[34] J.J. Gebhardt, J.M. Berry, Mechanical Properties of Pyrolytic Graphite. Aiaa Journal 3 (1965) 302-308.

[35] S. Wang, G. Chen, H. Huang, S. Ma, H. Xu, Y. He, J. Zou, Vapor-phase synthesis, growth mechanism and thickness-independent elastic modulus of single-crystal tungsten nanobelts. Nanotechnology 24 (2013) 505705.

[36] U. Ozgur, Y.I. Alivov, C. Liu, A. Teke, M.A. Reshchikov, S. Dogan, V. Avrutin, S.J. Cho, H. Morkoc, A comprehensive review of ZnO materials and devices. J. Appl. Phys. 98 (2005) 041301.

[37] A. Roy, H. Xie, S. Wang, H. Huang, The kinetic friction of ZnO nanowires on amorphous SiO2 and SiN substrates. Appl. Surf. Sci. 389 (2016) 797-801.

[38] E. Koren, E. Lörtscher, C. Rawlings, A.W. Knoll, U. Duerig, Adhesion and friction in mesoscopic graphite contacts. Science 348 (2015) 679-683.

[39] H.K. Christenson, Adhesion and Surface-Energy of Mica in Air and Water. J. Phys. Chem. 97 (1993) 12034-12041.

[40] Y. Tian, N. Pesika, H.B. Zeng, K. Rosenberg, B.X. Zhao, P. McGuiggan, K. Autumn, J. Israelachvili, Adhesion and friction in gecko toe attachment and detachment. Proc. Natl. Acad. Sci. U. S. A. 103 (2006) 19320-19325.

[41] L. Xu, M. Salmeron, Effects of surface ions on the friction and adhesion properties of mica. Langmuir 14 (1998) 2187-2190.

[42] S. Ohnishi, A.M. Stewart, Humidity Dependence of Interfacial Friction between Mica Surfaces. Langmuir 18 (2002) 6140-6146.

[43] H. Lee, J.H. Ko, J.S. Choi, J.H. Hwang, Y.H. Kim, M. Salmeron, J.Y. Park, Enhancement of Friction by Water Intercalated between Graphene and Mica. J Phys Chem Lett 8 (2017) 3482-3487.

[44] Z. Liu, J.R. Yang, F. Grey, J.Z. Liu, Y.L. Liu, Y.B. Wang, Y.L. Yang, Y. Cheng, Q.S. Zheng, Observation of Microscale Superlubricity in Graphite. Phys. Rev. Lett. 108 (2012) 205503.

[45] H. Li, J. Wang, S. Gao, Q. Chen, L. Peng, K. Liu, X. Wei, Superlubricity between MoS2 Monolayers. Adv. Mater. 29 (2017) 1701474.

[46] C. Lee, Q. Li, W. Kalb, X.-Z. Liu, H. Berger, R.W. Carpick, J. Hone, Frictional Characteristics of Atomically Thin Sheets. Science 328 (2010) 76-80.

Table 1. Interfacial friction between atomically smooth surfaces

Interfacial systems A-B	Testing conditions	Frictional shear stress/ Force (MPa/nN)	Measured Ratios	Combining Relationships
ZnO-mica (this work)	Ambient atmosphere (50 - 55% RH)	$\tau_{ZnO-M} = 5.1$	$\frac{\tau_{ZnO-M}}{\tau_{ZnO-G}} = 10$	
ZnO-graphite (this work)		$\tau_{ZnO-G} = 0.51$		
Si-mica [43]	Ambient atmosphere (45 - 50% RH)	–	$\frac{\tau_{Si-M}}{\tau_{Si-G}} = 10$	$\frac{\tau_{ZnO-M}}{\tau_{ZnO-G}} \approx \frac{\tau_{Si-M}}{\tau_{Si-G}} \approx \sqrt{\frac{\tau_{M-M}}{\tau_{G-G}}}$
Si-graphite [43]		–		
Mica-mica [42]	Ambient atmosphere (50 - 55% RH)	$\tau_{M-M} \sim 7.5$	$\sqrt{\frac{\tau_{M-M}}{\tau_{G-G}}} \approx 12$	
Graphite-graphite[38]	Ambient atmosphere	$\tau_{G-G} \sim 0.05$		
Sb-MoS_2 [28]	High vacuum	$\tau_{Sb-MoS_2} \sim 1$	$\frac{\tau_{Sb-MoS_2}}{\tau_{Sb-G}} \approx 1$	
Sb-graphite [16]		$\tau_{Sb-G} = 1.04$		
Si-MoS_2 [46]	Ambient atmosphere	$F_{Si-MoS_2} = 1$	$\frac{\tau_{Si-MoS_2}}{\tau_{Si-G}} = 1$	$\frac{\tau_{Sb-MoS_2}}{\tau_{Sb-G}} \approx \frac{\tau_{Si-MoS_2}}{\tau_{Si-G}} \approx \sqrt{\frac{\tau_{MoS_2-MoS_2}}{\tau_{G-G}}}$
Si-graphite [46]		$F_{Si-G} = 1$		
MoS_2-MoS_2 [45]	High vacuum (SEM chamber)	$\tau_{MoS_2-MoS_2} = 0.02 - 0.06$	$\sqrt{\frac{\tau_{MoS_2-MoS_2}}{\tau_{G-G}}} \approx 1$	
Graphite-graphite[44]	Vacuum (SEM chamber)	$\tau_{G-G} = 0.02 - 0.04$		

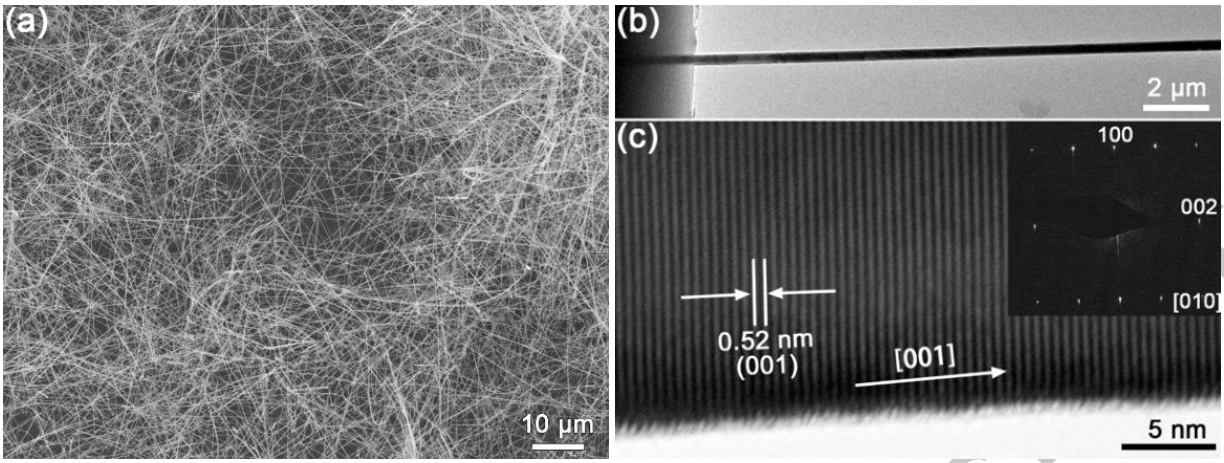

Fig. 1. (a) Low magnification SEM image of ZnO NWs. (b) Typical TEM and and (c) the corresponding high-resolution TEM images of ZnO NWs. The inset in (c) shows the corresponding selected-area electron diffraction pattern.

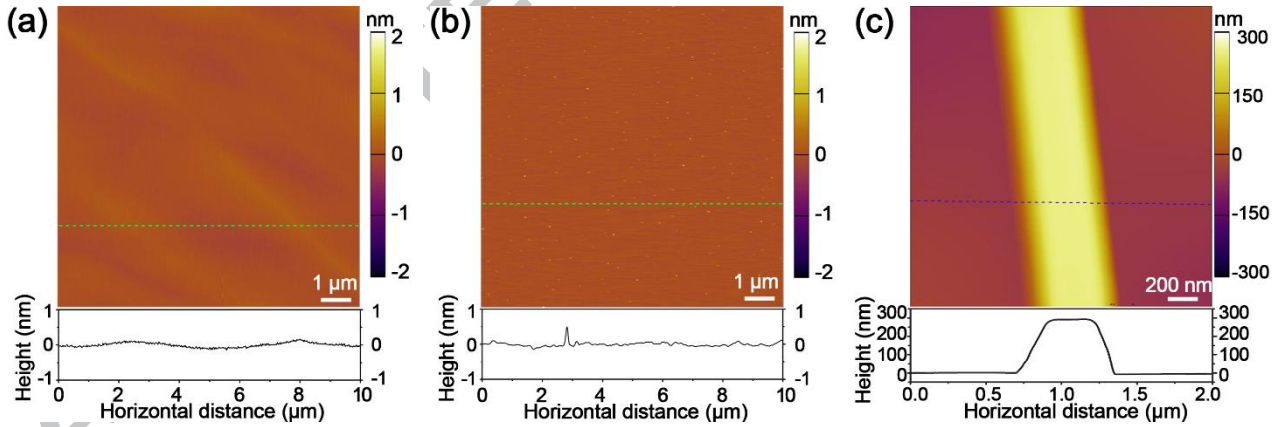

Fig. 2. Two-dimensional AFM micrographs and line-profiles: (a) graphite substrate, (b) mica substrate, and (c) ZnO NW.

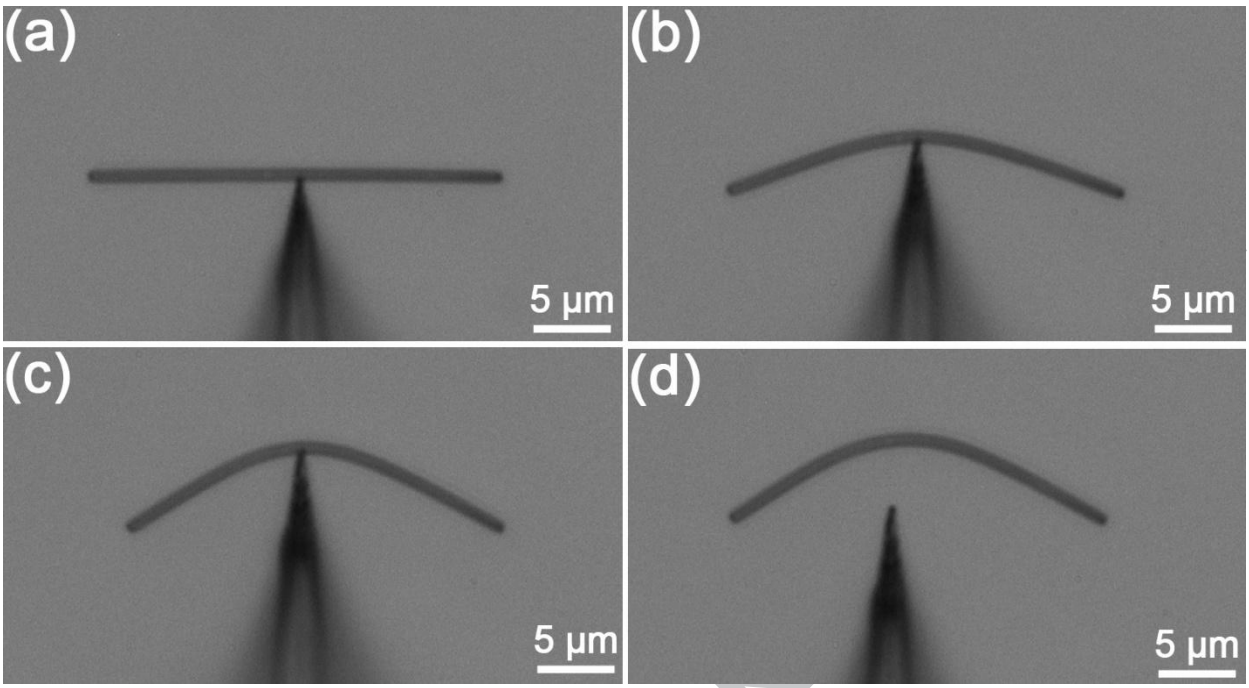

Fig. 3. Typical bent shapes of the same ZnO NW on the graphite substrate captured by the optical microscope in the mid-point push test: (a) prior to sliding, (b) sliding before the steady state, (c) sliding in the steady state, (d) after the tip withdrawal.

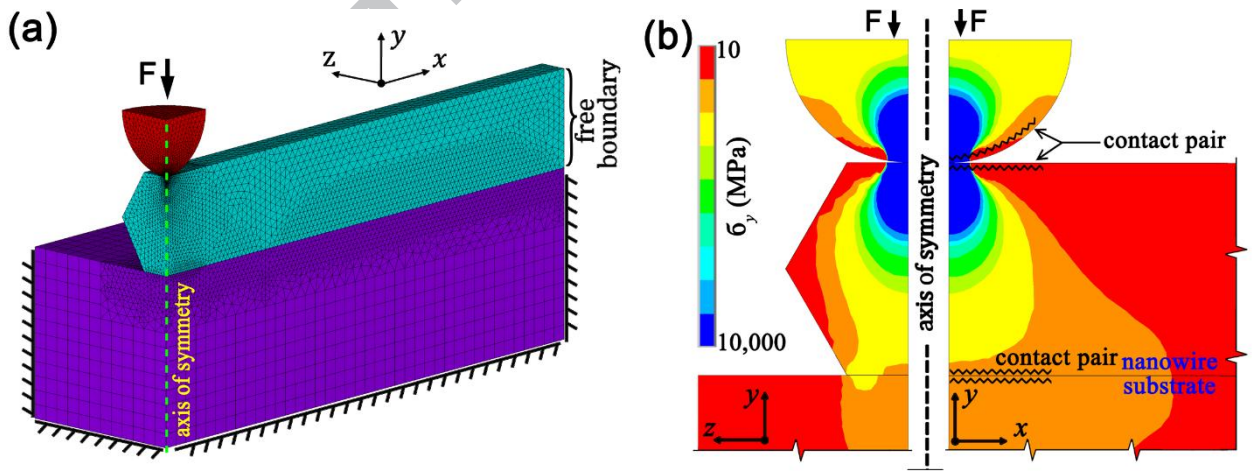

Fig. 4. (a) Isometric view of axisymmetric FEA model of tip-NW-substrate system. (b) Contour plots of the normal compressive stress induced within a NW by a normal tip load, in both the *y*-*z* and *x*-*y* symmetry planes intersecting the midpoint of the NW. The location of the Hertzian contact surfaces are demarcated.

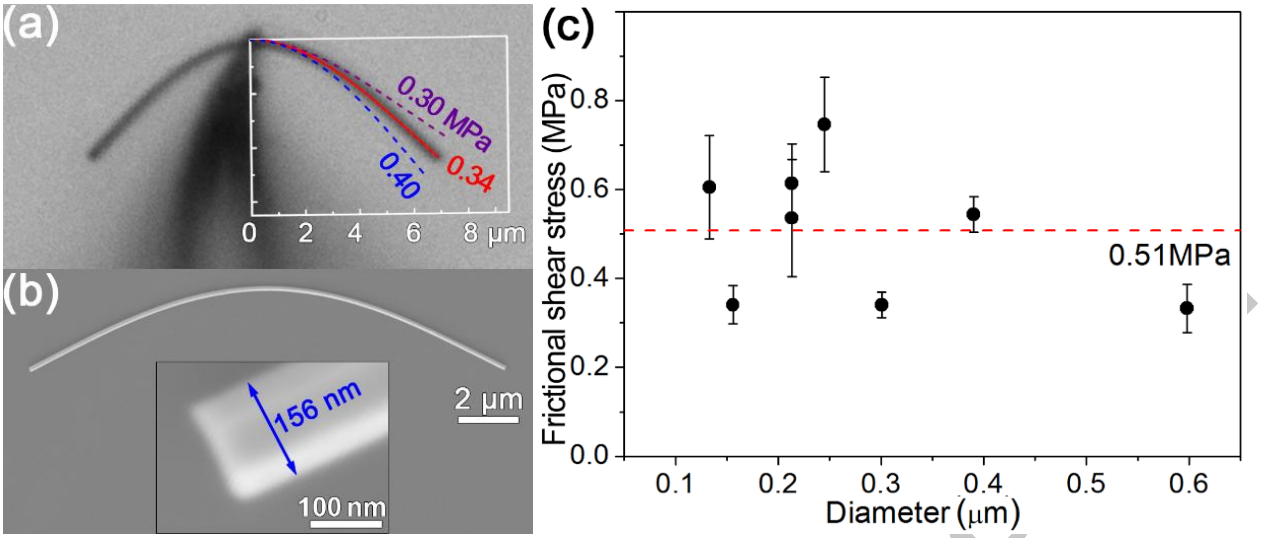

Fig. 5. (a) Optical image of a ZnO NW sliding stably on the grapphite substrate in the midpoint test. The three dotted lines are the modelled NW profiles using the frictional shear stresses of 0.30, 0.34 and 0.40 MPa, respectively. (b) SEM image of the ZnO NW in (a) after the test. The inset in (b) shows the hexagonal structure of the NW. (c) The kinetic stresses of ZnO NWs on graphite substrate plotted as a function of the diameter of NWs, where the errors were calculated from the uncertainties in the deflections, and the diameters and lengths of NWs obtained by OM and SEM, respectively.

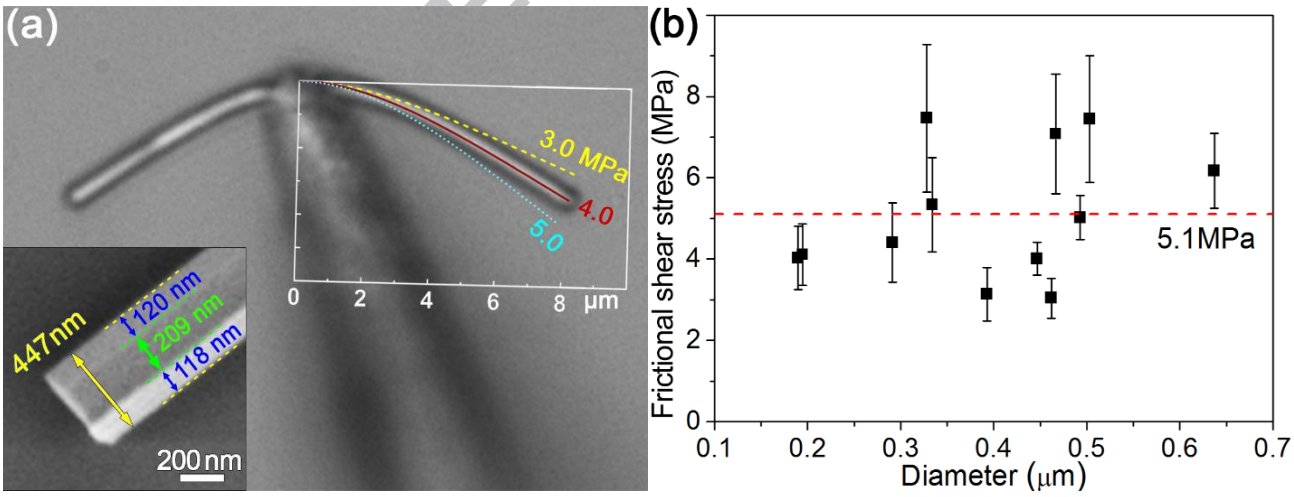

Fig. 6. (a) Optical image of a ZnO NW sliding stably on the mica substrate. The three dotted lines are the modelled NW profiles using the frictional shear stresses of 3.0, 4.0 and 5.0 MPa, respectively. The SEM image inset in (a) shows the hexagonal structure and diameter of the ZnO NW. (b) The kinetic stresses of ZnO NWs on mica substrate plotted as a function of the diameter of NWs, where the errors were calculated from the uncertainties in the deflections, and the diameters and lengths of the NWs obtained by OM and SEM, respectively.

Highlights

Frictional shear stress between ZnO nanowires and graphite substrate is 0.51 MPa.

Frictional shear stress between ZnO nanowires and mica substrate is 5.1 MPa.

Kinetic friction may not be dominated by adhesion at nanowire/substrate interfaces.

Two empirical equations were proposed to explain phenomenologically the results.